Hindawi Publishing Corporation
International Journal of Spectroscopy
Volume 2010, Article ID 627571, 6 pages
doi:10.1155/2010/627571

*Research Article*

# Absorption Line Profile of the $^5S_2^o$–$^5P_1$ Transition of Atomic Oxygen and Its Application to Plasma Monitoring

**K. Sasaki,[1] Y. Okumura,[2] and R. Asaoka[2]**

[1] *Plasma Nanotechnology Research Center, Nagoya University, Nagoya 464-8603, Japan*
[2] *Department of Electrical Engineering and Computer Science, Nagoya University, Nagoya 464-8603, Japan*

Correspondence should be addressed to K. Sasaki, sasaki@nuee.nagoya-u.ac.jp

Received 15 April 2009; Accepted 27 May 2009

Academic Editor: Roland Stamm



The line profile of the $^5S_2^o$–$^5P_1$ transition of atomic oxygen was measured by diode laser absorption spectroscopy. As a result, it was found that the absorption line profile had a wing component in the wavelength range detuned from the line center and was not fitted with a Gaussian function. The wing component was considered to be originated from dissociative excitation of molecular oxygen. We fitted the absorption line profile with the superposition of two Gaussian functions corresponding to high and low translational temperatures. We propose that the ratio of the high-temperature to low-temperature components is useful for monitoring the relative degree of dissociation of molecular oxygen in oxygen-containing plasmas. The ratio of the high-temperature to low-temperature components was compared with the survival ratio of molecular oxygen, which was evaluated from the lifetime of O($^5S_2^o$) in the afterglow of pulsed discharges.

## 1. Introduction

Low-pressure plasmas with electron densities below $10^{13}$ cm$^{-3}$ are widely used for various material processing such as dry etching and plasma-enhanced chemical vapor deposition. The spectral line profiles of atoms and molecules in low-pressure, low-density plasmas are governed by Doppler broadening, which represents the velocity distribution function of atoms and molecules in plasmas. Since collisions among neutral species in plasmas used for material processing are frequent, it is expected that the velocity distribution functions of atoms and molecules are approximated by Maxwellian functions with widths corresponding to the species temperatures. However, there are several processes which deviate the velocity distribution functions of neutral species from Maxwellian functions.

Spectral profiles of hydrogen Balmer lines have been investigated intensively by optical emission spectroscopy, and many authors have reported the existence of large Doppler broadening in their spectral line profiles [1–10]. The existence of large Doppler broadening means that the velocity distribution function of emitting species contains a high-energy component. A possible mechanism for the production of the high-energy component is collision between molecular hydrogen and ions. Another process for explaining the existence of the high-energy component is dissociative excitation of molecular hydrogen. This is because electron impact dissociation of a diatomic molecule is divided into two steps. The first step is electron impact excitation to an electronic state having a repulsive potential curve without changing the distance between nuclei. The second step is automatic separation of nuclei along the repulsive potential curve. Since the energy of the dissociated state is lower than that of the repulsive potential curve immediately after electron impact excitation, atoms produced after dissociation have kinetic energies corresponding the energy difference.

A reason why the investigations of the spectral line profiles are concentrated in atomic hydrogen may be the smallest mass number. Since the spectral resolution of optical emission spectroscopy is not high, atomic hydrogen, which has the widest Doppler broadening width (the smallest mass number), is suitable for investigating the spectral line profile by optical emission spectroscopy. In this work, we examined the spectral line profile of the $^5S_2^o$–$^5P_1$ transition of atomic oxygen by diode laser absorption spectroscopy. Since diode laser absorption spectroscopy has a much finer resolution than optical emission spectroscopy, we can examine the detailed structure of the spectral line profile. In addition, we propose a method for monitoring the relative degree of dissociation of molecular oxygen in oxygen-containing discharges from the spectral line profile of the $^5S_2^o$–$^5P_1$ transition. The plasma processing industry requires a simple, economical technique which is applicable to the monitoring of plasma processing tools. The proposed method has a potential as a plasma monitoring tool because of the compactness, simplicity, and the economical price of a diode laser.

## 2. Experiment

The plasma source and the system for diode laser absorption spectroscopy are the same as those used in a previous work [11], where we evaluated the gas temperatures in hydrogen plasmas from the absorption line profile of the Balmer-$\alpha$ line. We used pure oxygen at pressures from 30 to 100 mTorr for discharge in this experiment. Helicon-wave plasmas were produced by applying rf power at 13.56 MHz to a helical antenna wound around a glass discharge tube of 1.6 cm inner diameter. The plasma column with the same diameter as the glass tube was confined radially by the uniform magnetic field along the cylindrical axis of a vacuum chamber. The strength of the magnetic field was adjusted to be 70 G to avoid the distortion of the spectral line profile due to the Zeeman effect. The plasmas were produced in a pulsed mode with a discharge duration of 40 milliseconds and a repetition frequency of 2 Hz to avoid the overheating of the plasma source.

A commercial diode laser (TOPTICA, DL100) beam was injected into the plasma from the radial direction of the cylindrical vacuum chamber. The wavelength of the diode laser beam was tuned around the line center of the $^5S_2^o$–$^5P_1$ transition (777.539 nm). The tuning of the laser wavelength was triggered at 15 milliseconds after the initiation of the pulsed discharge, when the plasma reached the steady-state condition. Sweeping the laser wavelength for ±20 pm needed 20 milliseconds. The wavelength tuning of the diode laser beam was monitored using a spectrum analyzer. The power of the diode laser beam was attenuated below 10 $\mu$W to avoid saturation. The laser beam transmitted through the plasma was detected using a photomultiplier tube via a monochromator.

## 3. Absorption Line Profile and the Interpretation

For the sake of comparison, we produced an argon plasma and measured the absorption line profile of the $4s[3/2]_2^o$–$4p[3/2]_2$ transition at a wavelength of 763.510 nm. Figure 1 shows the absorption line profile of the $4s[3/2]_2^o$–$4p[3/2]_2$ transition observed at an argon pressure of 30 mTorr and an rf power of 1.5 kW. The open circles illustrated in Figure 1(a) represent the experimental result, and the solid curve shows the data fitting using a Gaussian function corresponding to a temperature of 0.066 eV. Figure 1(b) shows the difference between the experimental result and the data fitting. The difference

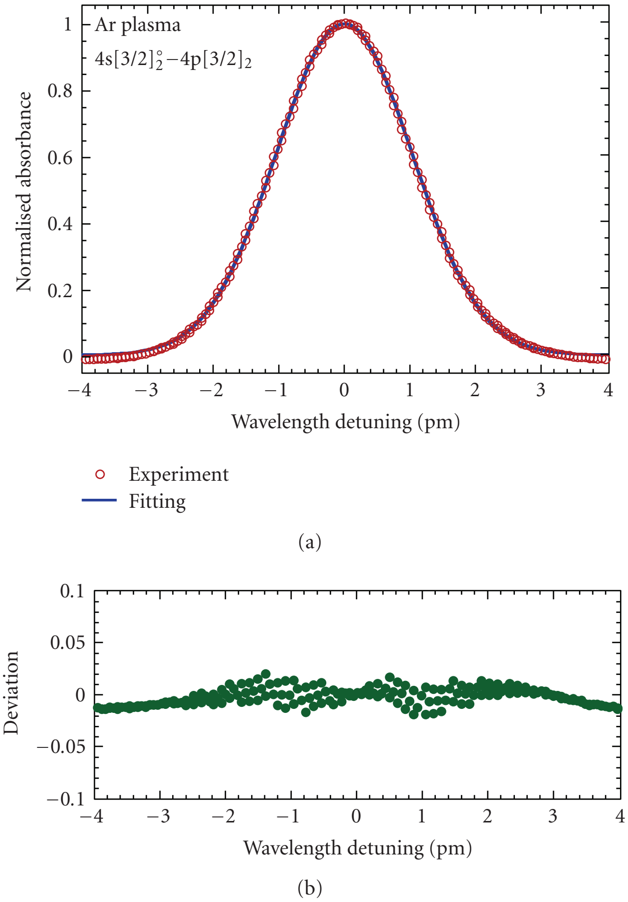


Figure 1: Absorption line profile of the $4s[3/2]_2^o$–$4p[3/2]_2$ transition of argon observed at an rf power of 1.5 kW and a pressure of 30 mTorr. The open circles illustrated in (a) show the experimental result, and the solid curve is the data fitting using a Gaussian function with a temperature of 0.066 eV. The difference between the experimental result and the data fitting is shown in (b).

shown in Figure 1(b) is fairly small, and the absorption line profile of the $4s[3/2]_2^o$–$4p[3/2]_2$ transition was approximated well by a Gaussian function.

Figure 2 shows the absorption line profile of the $^5S_2^o$–$^5P_1$ transition of atomic oxygen observed in an oxygen plasma produced at an oxygen pressure of 30 mTorr and an rf power of 1.5 kW. The solid curve shown in Figure 2(a) represents a Gaussian profile corresponding to a temperature of 0.12 eV. It is clearly understood from Figure 2 that the absorption line profile of the $^5S_2^o$–$^5P_1$ transition was not approximated by a Gaussian function. The comparison between the experimental result and the data fitting indicates that the velocity distribution function of the metastable $^5S_2^o$ state of atomic oxygen had a high-energy component. Figure 3 shows the data fitting of the same experimental absorption line profile with the superposition of two Gaussian functions corresponding to temperatures of 0.072 and 0.37 eV. The absorption line profile of the $^5S_2^o$–$^5P_1$ transition observed experimentally was approximated well by the superposition of two Gaussian functions.

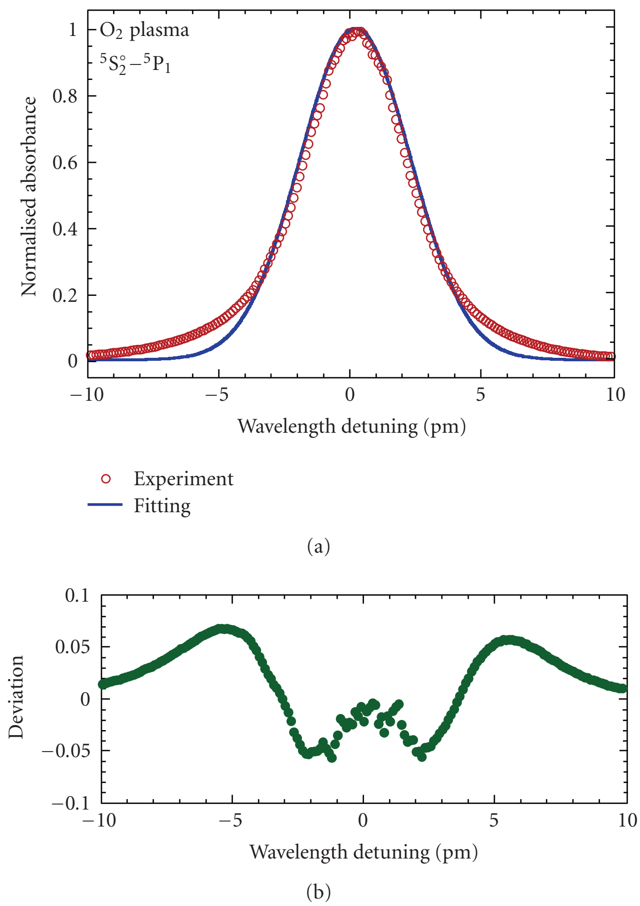


FIGURE 2: Absorption line profile of the $^5S_2^o$–$^5P_1$ transition of atomic oxygen observed at an rf power of 1.5 kW and a pressure of 30 mTorr. The open circles illustrated in (a) show the experimental result, and the solid curve is the data fitting using a Gaussian function with a temperature of 0.12 eV. The difference between the experimental result and the data fitting is shown in (b).

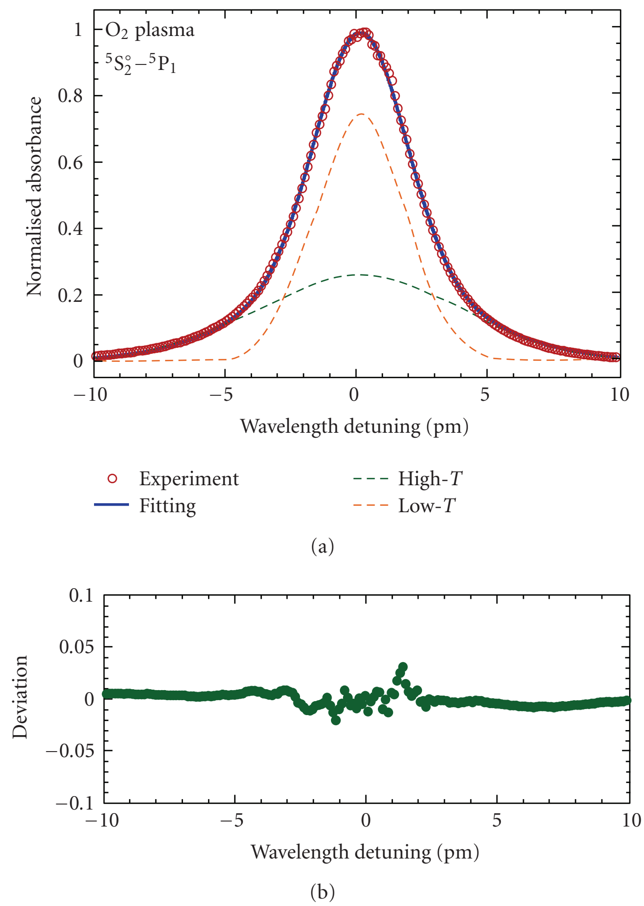


FIGURE 3: The same experimental absorption line profile as that shown in Figure 2 and the data fitting using the superposition of two Gaussian functions with temperatures of 0.072 and 0.37 eV. The difference between the experimental result and the data fitting is shown in (b).

There is a possibility that the temperatures of positive ions are higher than those of neutral species. In addition, there is a possibility that the velocity distribution function of positive ions has a high-energy component which is originated from the reflection of positive ions in the sheath. Therefore, charge exchange collision between positive ions and neutral species is a possible mechanism for the generation of the high-energy component in the velocity distribution function of neutral species. However, the experimental result that the absorption line profile of the $4s[3/2]_2^o$–$4p[3/2]_2$ transition of argon was approximated well by a Gaussian function indicates that the velocity distribution function of the metastable $4s[3/2]_2^o$ state of argon is thermalized completely, and the high-energy component originated from charge exchange collision is negligible in this plasma source.

A reasonable mechanism for explaining the high-energy component observed in the absorption line profile of the $^5S_2^o$–$^5P_1$ transition of atomic oxygen is dissociative excitation. In this interpretation of the spectral line profile, the low-energy component in the velocity distribution function of $O(^5S_2^o)$ is produced by the three-step process represented by

$$O_2 + e \longrightarrow O(^3P^o, \text{fast}) + O(^3P^o, \text{fast}) + e, \qquad (1)$$

$$O(^3P^o, \text{fast}) + M \longrightarrow O(^3P^o, \text{slow}) + M, \qquad (2)$$

$$O(^3P^o, \text{slow}) + e \longrightarrow O(^5S_2^o, \text{slow}) + e. \qquad (3)$$

Since the lifetime of $O(^3P^o)$ is much longer than the reciprocal of the collision frequency, the velocity distribution function of $O(^3P^o)$ is thermalized, and the high-energy component ($O(^3P^o, \text{fast})$ in (1)) becomes negligible via elastic collision processes (2). On the other hand, the high-energy component in the velocity distribution function of $O(^5S_2^o)$ is considered to be produced by dissociative excitation:

$$O_2 + e \longrightarrow O(^5S_2^o, \text{fast}) + O(^3P^o, \text{fast}) + e. \qquad (4)$$

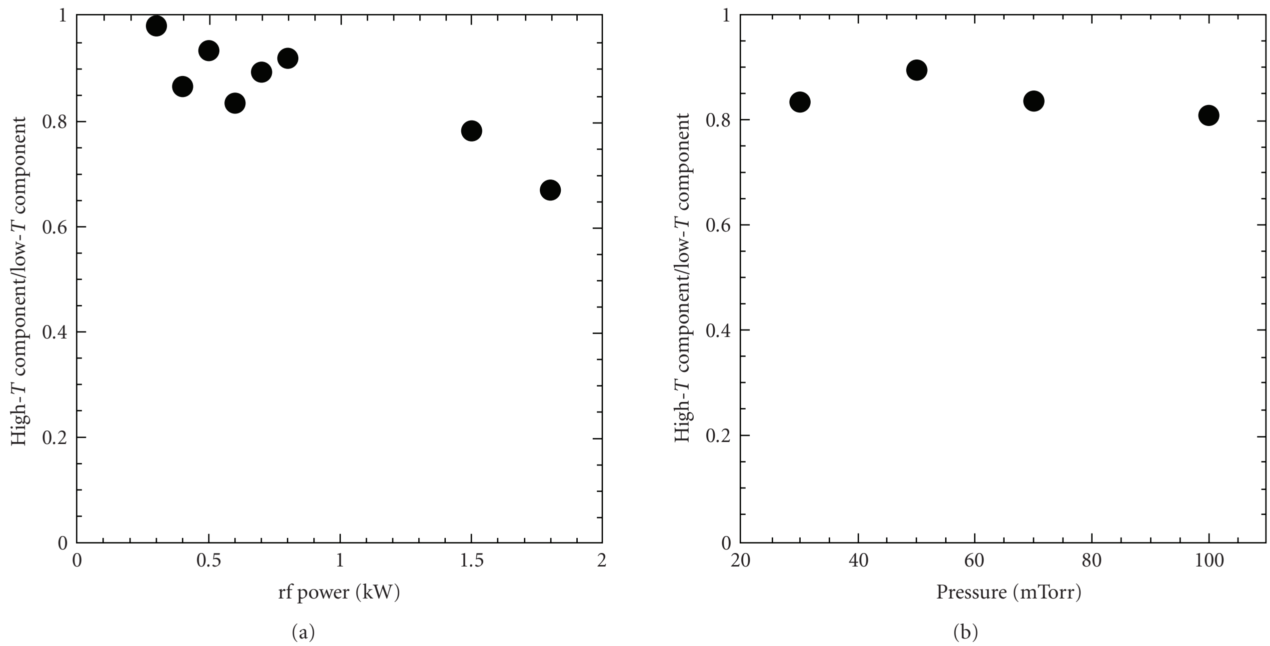


Figure 4: The density ratio of the high-temperature to low-temperature components as functions of (a) the rf power and (b) the oxygen pressure.

Since the lifetime of $O(^5S_2^o)$ is determined by the loss processes described below and is much shorter than the lifetime of $O(^3P^o)$, the high-energy component ($O(^5S_2^o, \text{fast})$ in (4)) is expected to survive in the velocity distribution function.

## 4. Application to the Monitoring of Degree of Dissociation

According to the aforementioned production processes, the densities of the slow (low-energy) and fast (high-energy) components in the velocity distribution function are given by

$$[O(^5S_2^o, \text{slow})] = \tau k_{\text{ex}}[O]n_{\text{e}}, \quad (5)$$

$$[O(^5S_2^o, \text{fast})] = \tau k_{\text{diss}}[O_2]n_{\text{e}}, \quad (6)$$

respectively, where $\tau$ is the lifetime of $O(^5S_2^o)$, $n_{\text{e}}$ is the electron density, and [X] stands for the density of species X. The rate coefficients for (3) and (4) are represented by $k_{\text{ex}}$ and $k_{\text{diss}}$, respectively. Therefore, the density ratio of molecular oxygen to atomic oxygen is evaluated by

$$\frac{[O_2]}{[O]} = \frac{k_{\text{ex}}}{k_{\text{diss}}} \frac{[O(^5S_2^o, \text{fast})]}{[O(^5S_2^o, \text{slow})]}. \quad (7)$$

The relative values of $[O(^5S_2^o, \text{slow})]$ and $[O(^5S_2^o, \text{fast})]$ are estimated by integrating the two Gaussian functions with low and high temperatures in the absorption line profile of the $^5S_2^o{-}^5P_1$ transition, respectively. Hence, if we ignore the variation of $k_{\text{ex}}/k_{\text{diss}}$ with respect to the

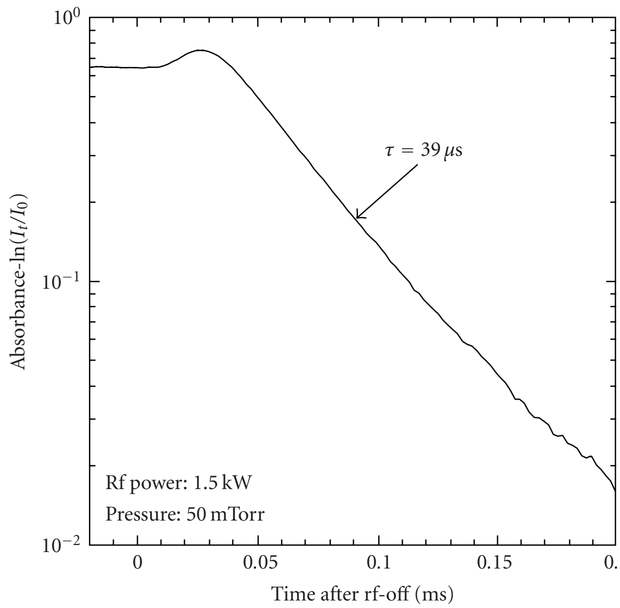


Figure 5: Temporal variation of the absorbance at the line center of the $^5S_2^o{-}^5P_1$ transition in the afterglow phase of a pulsed discharge at an rf power of 1.5 kW and a pressure of 50 mTorr.

discharge conditions, the relative variation of $[O_2]/[O]$ is roughly evaluated by $[O(^5S_2^o, \text{fast})]/[O(^5S_2^o, \text{slow})]$. We evaluated $[O(^5S_2^o, \text{fast})]$ and $[O(^5S_2^o, \text{slow})]$ at various discharge conditions from the absorption line profiles. The ratio $[O(^5S_2^o, \text{fast})]/[O(^5S_2^o, \text{slow})]$ is plotted in Figure 4 as functions of the rf power and the discharge pressure.

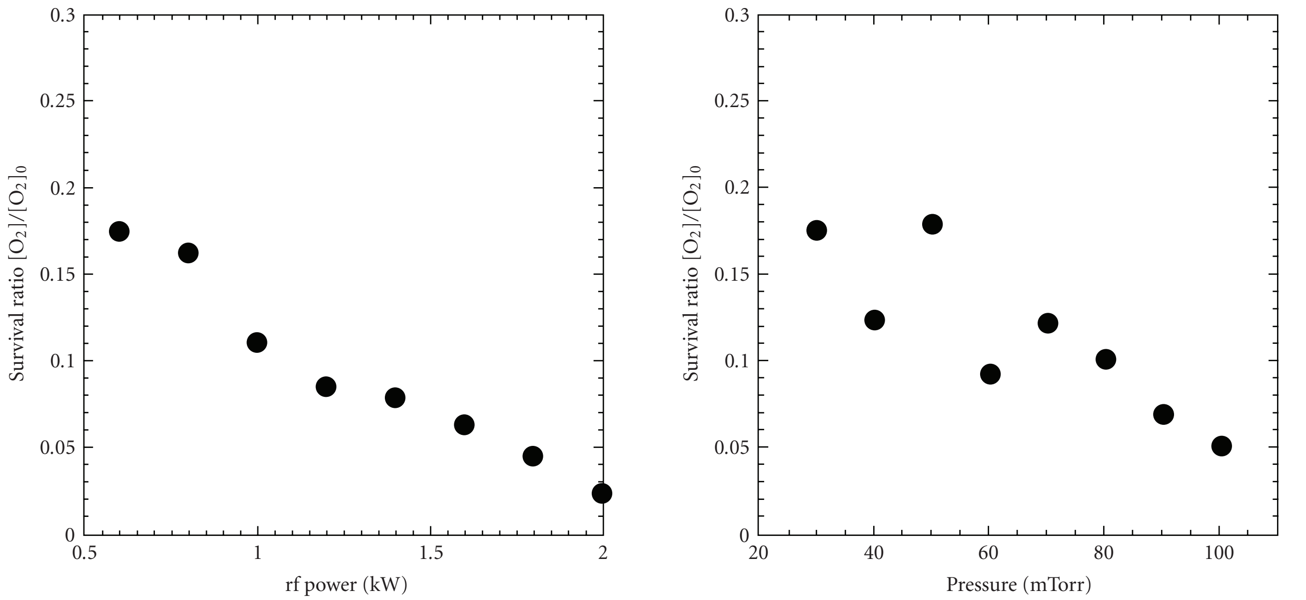


(a) (b)

Figure 6: Survival ratio of $O_2$ as functions of (a) the rf power and (b) the oxygen pressure. The $O_2$ density before discharge ($[O_2]_0$) was evaluated from the gas pressure, and the survived $O_2$ density ($[O_2]$) was evaluated from the lifetime of $O(^5S_2^o)$ in the afterglow phase.

## 5. Comparison with Degree of Dissociation Evaluated from Lifetime of $O(^5S_2^o)$

The major loss processes of $O(^5S_2^o)$ are diffusion, spontaneous emission, and collisional quenching with $O_2$, and the lifetime $\tau$ in (5) and (6) are given by

$$\frac{1}{\tau} = k_q[O_2] + \frac{1}{\tau_d} + \frac{1}{\tau_r}, \tag{8}$$

where $k_q$ is the rate coefficient for collisional quenching, $\tau_d$ is the diffusion time constant, and $\tau_r$ is the radiative lifetime. The values of $k_q$ and $1/\tau_r$ are given in literature [12, 13] as $k_q = 2.2\times10^{-10}\,\text{cm}^3/\text{s}$ and $1/\tau_r = 5.6\times10^3\,\text{s}^{-1}$. The diffusion time constant of O atoms in $O_2$ plasmas produced in the plasma source used in this experiment has been examined in a previous work and was estimated as $1/\tau_D < 2\times10^3\,\text{s}^{-1}$ at pressures higher than 30 mTorr [14, 15]. Therefore, the dominant term in the right-hand side of (8) is $k_q[O_2]$, and the $O_2$ density can be estimated by measuring the lifetime of $O(^5S_2^o)$.

Figure 5 shows the temporal variation of the absorbance at the line center ($-\ln(I_t/I_0)$ with $I_0$ and $I_t$ being the incident and transmitted laser intensities, resp.) in the afterglow phase of a pulsed discharge at an rf power of 1.5 kW and a pressure of 50 mTorr. The slight increase in the absorbance immediately after the termination of the rf power may be due to the production of $O(^5S_2^o)$ by recombination reactions. After that, the absorbance decreased exponentially as shown in Figure 5, and the decay time constant was evaluated to be $\tau = 39$ microseconds, corresponding to $[O_2] \simeq 1.2\times10^{14}\,\text{cm}^{-3}$. Since the $O_2$ density before the discharge was $[O_2]_0 = 1.6\times10^{15}\,\text{cm}^{-3}$, the survival ratio of $O_2$ in the discharge was evaluated to be $[O_2]/[O_2]_0 \simeq 0.07$.

The survival ratio of $O_2$ thus evaluated is plotted in Figure 6 as functions of the rf power and the pressure. It is reasonable that the survival ratio decreases with the rf power as shown in Figure 6(a). The ratio of $[O(^5S_2^o,\text{fast})]/[O(^5S_2^o,\text{slow})]$ shown in Figure 4(a) also decreases with the rf power. Hence, the monitoring of the relative degree of dissociation from the absorption line profile of the $^5S_2^o$–$^5P_1$ transition is expected to work rather nicely, provided that a smaller survival ratio of $O_2$ directly means a higher O atom density. On the other hand, according to Figure 6(b), the survival ratio of $O_2$ decreases with the pressure, while the ratio of $[O(^5S_2^o,\text{fast})]/[O(^5S_2^o,\text{slow})]$ shown in Figure 4(b) is roughly constant. A possible explanation for this discrepancy is the increase in $k_{ex}/k_{diss}$ in (7) with the pressure. This is because $k_{ex}/k_{diss}$ decreases with the electron temperature since the threshold electron energy for (4) is higher than that for (3). Since the electron temperature is usually a decreasing function of the pressure, it is expected that the decrease in the survival ratio of $O_2$ is compensated by the increase in $k_{ex}/k_{diss}$, resulting in the roughly constant $[O(^5S_2^o,\text{fast})]/[O(^5S_2^o,\text{slow})]$ with the pressure. Further investigation is necessary to evaluate the discharge conditions where this method is applicable.

## 6. Conclusions

In this work, we investigated the absorption line profile of the $^5S_2^o$–$^5P_1$ transition of atomic oxygen by diode laser absorption spectroscopy. The Doppler broadened absorption line profile had a wing component corresponding to a high-energy tail in the velocity distribution function of the metastable $^5S_2^o$ state and was fitted by the superposition of two Gaussian functions with high and low temperatures. The comparison with the absorption line profile of the $4s[3/2]_2^o$–$4p[3/2]_2$ transition of argon suggests that the origin of the high-energy component in the absorption line profile of the ${}^5S_2^o$–${}^5P_1$ transition is electron impact dissociative excitation of $O_2$. We propose a method for monitoring the relative degree of dissociation of $O_2$ by the ratio of the high-temperature to low-temperature components in the absorption line profile. The relative degree of dissociation estimated by the proposed method was compared with the survival ratio of $O_2$ evaluated from the lifetime of the ${}^5S_2^o$ state. As a result, a reasonable agreement was obtained in the rf power dependence of the relative degree of dissociation, but the agreement was insufficient in the pressure dependence.

## References

[1] K. Ito, N. Oda, Y. Hatano, and T. Tsuboi, "Doppler profile measurements of balmer-$\alpha$ radiation by electron impact on $H_2$," *Chemical Physics*, vol. 17, no. 1, pp. 35–43, 1976.

[2] R. S. Freund, J. A. Schiavone, and D. F. Brader, "Dissociative excitation of $H_2$: spectral line shapes and electron impact cross sections of the Balmer lines," *The Journal of Chemical Physics*, vol. 64, no. 3, pp. 1122–1127, 1976.

[3] G. Baravian, Y. Chouan, A. Ricard, and G. Sultan, "Doppler-broadened $H_\alpha$ line shapes in a rf low-pressure $H_2$ discharge," *Journal of Applied Physics*, vol. 61, no. 12, pp. 5249–5253, 1987.

[4] T. Ogawa, N. Yonekura, M. Tsukada, et al., "Electron-impact dissociation of water as studied by the angular difference doppler profiles of the excited hydrogen atom," *Journal of Physical Chemistry*, vol. 95, no. 7, pp. 2788–2792, 1991.

[5] S. A. Bzenic, S. B. Radovanov, S. B. Vrhovac, Z. B. Velikic, and B. M. Jelenkovic, "On the mechanism of Doppler broadening of $H_\beta$ after dissociative excitation in hydrogne glow discharges," *Chemical Physics Letters*, vol. 184, no. 1–3, pp. 108–112, 1991.

[6] J. M. Ajello, S. M. Ahmed, and X. Liu, "Line profile of H Lyman-$\beta$ emission from dissociative excitation of $H_2$," *Physical Review A*, vol. 53, no. 4, pp. 2303–2308, 1996.

[7] M. Andrieux, J. M. Badie, M. Ducarroir, and C. Bisch, "The evolution of the translational energy of hydrogen atoms in a 2 MHz inductively coupled plasma deposition reactor," *Journal of Physics D*, vol. 31, no. 12, pp. 1457–1464, 1998.

[8] O. P. Makarov, J. M. Ajello, P. Vattipalle, I. Kanik, M. C. Festou, and A. Bhardwaj, "Kinetic energy distributions and line profile measurements of dissociation products of water upon electron impact," *Journal of Geophysical Research A*, vol. 109, no. A9, article A09303, 2004.

[9] J. Jovović, N. M. Šišović, and N. Konjević, "Doppler spectroscopy of hydrogen Balmer lines in a hollow cathode water vapour and argon-water vapour glow discharge," *Journal of Physics D*, vol. 41, Article ID 235202, 2008.

[10] J. Kipritidis, J. Khachan, M. Fitzgerald, and O. Shrier, "Absolute densities of energetic hydrogen ion species in an abnormal hollow cathode discharge," *Physical Review E*, vol. 77, no. 6, Article ID 066405, 9 pages, 2008.

[11] M. Aramaki, Y. Okumura, M. Goto, S. Muto, S. Morita, and K. Sasaki, "Measurements of gas temperature in high-density helicon-wave $H_2$ plasmas by diode laser absorption spectroscopy," *Japanese Journal of Applied Physics*, vol. 44, no. 9A, pp. 6759–6763, 2005.

[12] T. Mori, K. Kanou, K. Mizuta, T. Kuramasu, Y. Ishikawa, and S. Arai, "Reactions of highly excited oxygen atoms $(2p^3 3s, {}^5S)$ with simple gas molecules," *The Journal of Chemical Physics*, vol. 97, no. 12, pp. 9094–9098, 1992.

[13] NIST Atomic Spectra Database, http://physics.nist.gov/PhysRefData/ASD/index.html.

[14] J. Matsushita, K. Sasaki, and K. Kadota, "Dynamic variation of the sticking coefficient of oxygen atoms in helicon-wave excited high-density oxygen plasmas," *Japanese Journal of Applied Physics*, vol. 36, no. 7, pp. 4747–4751, 1997.

[15] R. C. Reid, J. M. Prausnitz, and T. K. Sherwood, *The Properties of Gases and Liquids*, McGraw-Hill, New York, NY, USA, 1977.

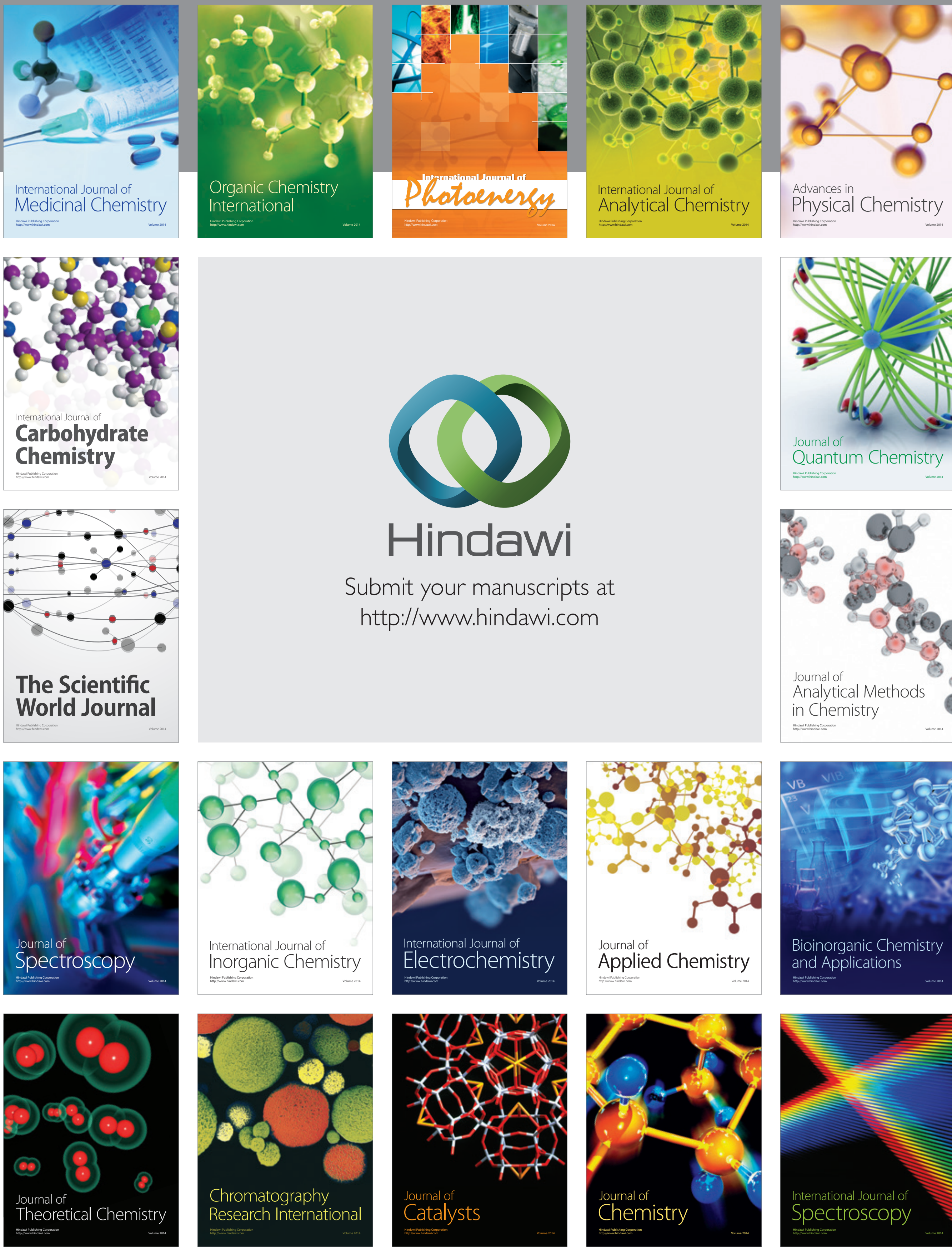
International Journal of Medicinal Chemistry
Organic Chemistry International
International Journal of Photoenergy
International Journal of Analytical Chemistry
Advances in Physical Chemistry
International Journal of Carbohydrate Chemistry
Hindawi
Submit your manuscripts at
http://www.hindawi.com
Journal of Quantum Chemistry
The Scientific World Journal
Journal of Analytical Methods in Chemistry
Journal of Spectroscopy
International Journal of Inorganic Chemistry
International Journal of Electrochemistry
Journal of Applied Chemistry
Bioinorganic Chemistry and Applications
Journal of Theoretical Chemistry
Chromatography Research International
Journal of Catalysts
Journal of Chemistry
International Journal of Spectroscopy